



Cite this: *Org. Biomol. Chem.*, 2022, **20**, 5254

Received 22nd April 2022,
Accepted 14th June 2022

DOI: 10.1039/d2ob00762b

rsc.li/obc

Self-assembly of a 5-fluorouracil and camptothecin dual drug dipeptide conjugate†

Yuan Sun, Cathleen M. Fry, Aileen Shieh, Xiangchen Cai, Thomas J. Reardon and Jon R. Parquette *

Nano-formulated, combinatory therapeutics that control the spatiotemporal aspects of drug release have potential to overcome many of the challenges faced in cancer therapy. Herein, we describe a peptide nanotube functionalized with two anticancer drugs, 5-fluorouracil (5-FU) and camptothecin (CPT). The nanotube was formed *via* peptide self-assembly, which positioned 5-FU on the surface at the aqueous interface; whereas, CPT was sequestered within the hydrophobic walls. Thus, two different release profiles were observed: rapid release of 5-FU, followed by slower, sustained production of CPT. This profile emerged from the rapid hydrolytic cleavage of 5-FU at the aqueous/nanotube interface, which produced a smaller nanotube comprised of the peptide fragment.

The delivery of combinations of anticancer drugs using nanotechnology-based carriers has emerged as an important strategy to effectively treat cancer.^{1,2} Delivery vehicles with nanoscale dimensions also benefit from the enhanced permeability and retention (EPR) effect, which allows the drugs to be delivered selectively into tumor cells.³ Combination therapy offers the potential to synergize multiple mechanisms of drug action, to reduce systemic toxicity and to suppress drug resistance.^{4–6} One strategy to coordinate the cellular uptake of multiple therapeutic agents relies on encapsulation within a single delivery vehicle, such as a liposomal or polymeric nanoparticle.^{7–9} However, formulating these systems using drugs with different physiochemical properties, such as size, charge and/or solubility, has been difficult and often produces systems exhibiting unpredictable release rates and noncoordinated biodistribution of the drugs.¹⁰ Covalent conjugation or modification to render the drugs more compatible with the vector have produced carriers with more precise ratiometric control over drug loading.^{11–14}

Department of Chemistry and Biochemistry, The Ohio State University, 100 W. 18th Ave., Columbus, Ohio 43210, USA. E-mail: parquette.1@osu.edu

† Electronic supplementary information (ESI) available. See DOI: <https://doi.org/10.1039/d2ob00762b>

The self-assembly of amphiphilic or peptidic drug derivatives provides another strategy to create delivery vehicles without the need for excipients.¹⁵ Carrier-free, nanoscale systems created by the self-assembly of two or more covalently-linked drugs offer the additional advantage of high loading, improved biocompatibility and the assurance of drug colocalization within the cell.^{16–23} The ability to tailor the amphiphilic monomers with hydrophilic and hydrophobic segments allows some of the difficulties of incorporating drugs with different physical properties to be overcome with proper design. These platforms often release each drug at a similar rate because loss of the first drug alters structure of the nanostructure building block, which leads to changes in the stability of the assembly.²⁴ In this work, we report the self-assembly of a dual drug peptide into a nanotube that hydrolytically releases 5-FU without loss of the nanotube structure, thereby allowing for slower, sustained release of CPT.

Combination therapy using irinotecan, a CPT analog, along with 5-FU has shown efficacy against gastrointestinal cancers.^{25–27} To explore the potential of combining two drugs with vastly different solubility into a single, self-assembled nanotube, we functionalized a dilysine peptide, *via* succinyl linkages, with 5-FU at the N-terminus, and with CPT at the ε-amino group of a lysine residue. In contrast to the hydrophobic nature of CPT, which exhibited low water solubility, the structure of 5-FU was hydrophilic and water soluble. We reasoned that the juxtaposition of the two drugs along the peptide backbone of **1** (Fig. 1) would create an amphiphilic structure capable of assembling *via* β-sheet interactions and hydrophobic sequestration of the CPT segment.^{28–30} Nanotube assembly in aqueous media would position the hydrophilic 5-FU group at the aqueous interface with the CPT molecule sequestered within the hydrophobic walls. This arrangement would be expected to permit the 5-FU to undergo hydrolytic release more rapidly than CPT. However, the remaining CPT-peptide fragment (**2**) would retain amphiphilicity due to the presence of the negatively charged succinate at the N-terminus. On that basis, we hypothesized that the nanotube

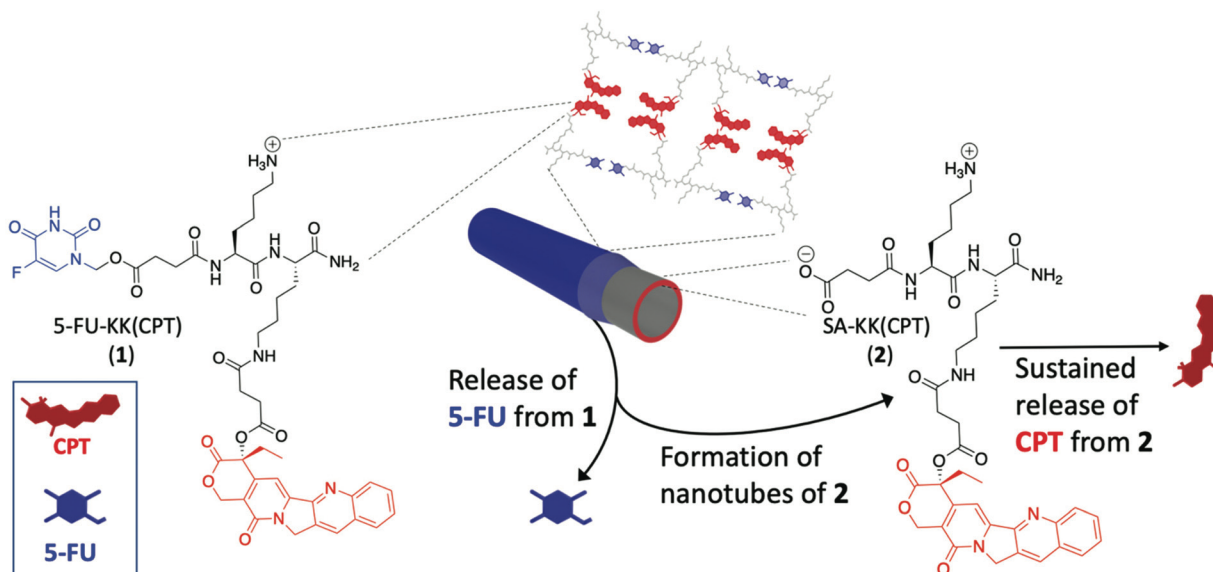


Fig. 1 Stepwise release of CPT and 5-FU from nanotubes, created by the self-assembly of 5-FU-KK(CPT) (1). Hydrolytic cleavage of 5-FU from 1 produces nanotubes of SA-KK(CPT) (2).

structure would remain intact following release of the 5-FU, which would permit slower, sustained release of CPT.

To evaluate the assembly characteristics of the peptide carrier prior to and following hydrolytic release of 5-FU, peptides 1 (5-FU-KK(CPT)) and 2 (SA-KK(CPT)) were prepared using standard Fmoc/t-Boc solid-phase peptide synthesis (Scheme S1†). CPT-peptide 2 would serve as the carrier of CPT upon initial hydrolytic release of 5-FU from 1. Accordingly, stepwise deprotection of the Fmoc and MTT groups of a dilysinopeptide backbone, followed by on-resin amidation allowed for the selective introduction of 5-Fu (1)/succinic acid (2), and CPT at the N-terminal and sidechain positions, respectively. The self-assembly of 1 and 2 was then explored by transmission electron microscopy (TEM) and UV-Vis/CD spectroscopy. Each peptide was incubated at a concentration of 10 (for 2) or 20 mM (for 1) in PBS for 72 h to induce self-assembly. After diluting to 1 mM, TEM imaging revealed the formation of an array of nanotubes from both peptides, showing average diameters of 84 ± 11 nm for 1 and 72 ± 11 nm for 2 (Fig. 2). The UV-Vis spectrum of 1 displayed absorption bands at 254 and 368 nm, corresponding to transitions of the 5-FU and CPT chromophores, respectively in PBS (Fig. 3a). The circular dichroism (CD) spectrum of 1 exhibited signals in the 230–280 and 350–400 nm ranges, overlapping with the absorption ranges of both drugs. In contrast, 2 exhibited only weak CD signals in PBS, indicative of comparatively weaker interactions between the CPT chromophores in the assembly. The small amount of red-shifting in CPT absorptions in the UV-Vis spectra, and the relatively weak CD signals of 1 and 2 indicated that the packing of the drugs within the nanotubes emanated primarily from hydrophobic effects, rather than well-defined π – π interactions.³¹ Deconvolution of the Fourier-transform infrared (FTIR) spectra in PBS (20 mM, D₂O) revealed amide I bands indicative of 86% (1) and 53% (2) β -sheet charac-

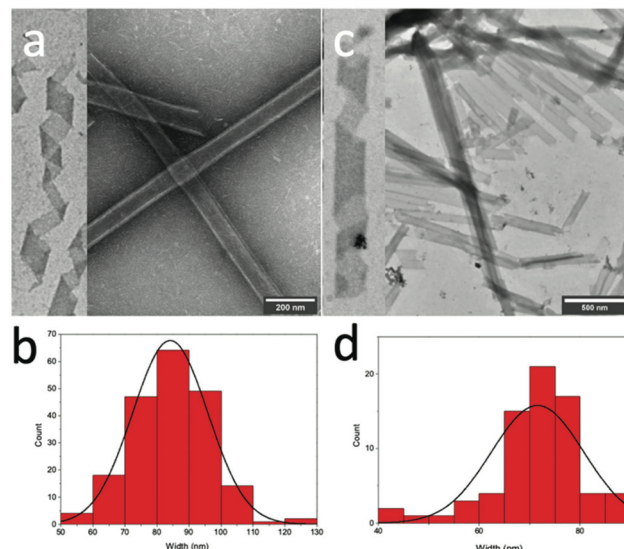


Fig. 2 TEM images and width distribution histograms of the nanotubes formed by 5-FU-KK(CPT) (1) (a and b) and SA-KK(CPT) (2) (c and d). The average diameters were 84 ± 11 nm and 72 ± 11 nm for 1 and 2, respectively. Samples were aged in PBS at 10 (for 2) or 20 mM (for 1) for 72 h and imaged on copper coated grids at 1 mM, stained with 2% uranyl acetate. TEM insets highlight helically coiled precursors to the nanotubes.

ter of the nanotube secondary structures (Fig. S12 and S13†).³² The critical aggregation concentrations (CAC) of the nanotubes were determined to be 5 μ M and 263 nM for 1 and 2, measured by recording the concentration dependence of the CPT fluorescence (Fig. S14 and S15†).^{33,34} These CAC values suggested that the stability of the nanotube increased after release of the 5-FU.

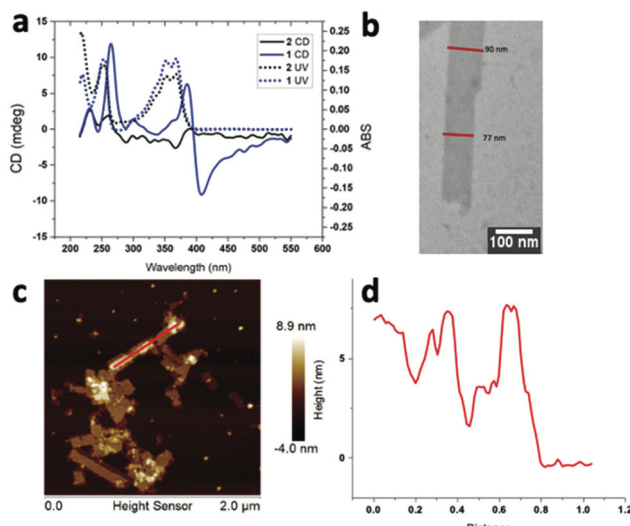


Fig. 3 (a) Co-plot of CD (solid lines) and UV (dotted lines) of **1** (blue) and **2** (black). Samples were aged in PBS (pH 7.4) at 10 mM for 72 h then diluted to 0.1 mM before analysis. (b) TEM images of **1**, assembled in PBS (pH 7.4) for 72 h at 10 mM, then diluted to 0.1 mM and heated to 37 °C for 72 h to induce drug release. Image shows regions of the nanotube with smaller diameters, consistent with hydrolytic release of 5-FU and the formation of nanotubes from **2**. (c) AFM images and (d) cross-sectional height analysis of **1** after drug release at 37 °C for 24 h at 0.1 mM. Samples were prepared by incubating **1** in PBS (pH 7.4) at 10 mM for 72 h, then diluting to 0.1 mM and heating at 37 °C for 24 h. Samples for TEM were stained with 2% uranyl acetate solution. AFM samples were deposited on a freshly cleaved, mica disk and analyzed in tapping mode.

The presence of helically coiled intermediates among the fully formed nanotubes of **1** and **2** in TEM images indicated that assembly proceeded *via* the coiling and lateral fusion of β -sheet ribbons (Fig. 2a/c, insets). AFM imaging of the nanotubes provided cross-sectional heights of 9–10 (**1**) and 5–6 nm (**2**), reflecting twice the thickness of the walls due to compression of the nanotube by the AFM tip (Fig. S18 and S19†). Thus, the extended dimensions of **1** (2.1×2.5 nm, Fig. S9†) and **2** (1.4×2.5 nm, Fig. S10†), suggested that the nanotube

walls of both structures were comprised of β -sheet bilayers of approximately two molecules, as shown in Fig. 1. Therefore, a structural model of nanotubes formed by **1** would sequester the hydrophobic CPT moieties within the bilayer wall with the hydrophilic 5-FU molecules projected toward the aqueous interface.

Hydrolytic release of 5-FU required initial cleavage of the acyloxymethylene linkage, followed by subsequent collapse of the resultant hemiaminal intermediate, whereas hydrolysis of the 20-O-succinyl linkage would release CPT from the nanotube carrier.^{35,36} The positioning of 5-FU at the surface of the nanotube exposes the ester linkage to the aqueous phase, and would portend a faster rate of hydrolytic release, compared to CPT. The release of both 5-FU and CPT were recorded by HPLC over 5 days in PBS and human serum (HS) at 37 °C at 0.1 mM and 1 mM (Fig. 4, S22–S24†). It is notable that the rate of 5-FU release was significantly higher than CPT in PBS, but the rate difference decreased at lower concentration. For example, whereas 90% of 5-FU was released after 48 h at 1 mM, only 15% of CPT had been released at the same time point. Although the amount of 5-FU released at 0.1 mM was similar (95%) after 48 h, the proportion of free CPT increased to 31%. Whereas, the release rate 5-FU was similar in human serum, CPT was released at a slightly higher rate compared with PBS. For example, 80% 5-FU and 44% CPT was produced after 40 h at 0.1 mM in HS. (Fig. S24†). The difference in the rate of release of 5-FU and CPT emerged from the selective shielding of CPT from the aqueous phase by the nanotube structure. At lower concentrations, a shift in the nanotube-monomer equilibrium toward the monomer state increased the release rate and decreased the rate difference between 5-FU and CPT.

Self-assembled nanocarriers with multiple, covalently bound drugs often release each drug at a similar rate because chemical cleavage of one drug reduces the stability of assembled structure. Although the concentration of **1** decreased rapidly upon exposure to PBS at 37 °C, concurrent with the release of free 5-FU and **2**, the amount of **2** remained reasonably stable over 120 h. The stability of **2**, and the slower extended release of CPT over time, emerged from the ability of

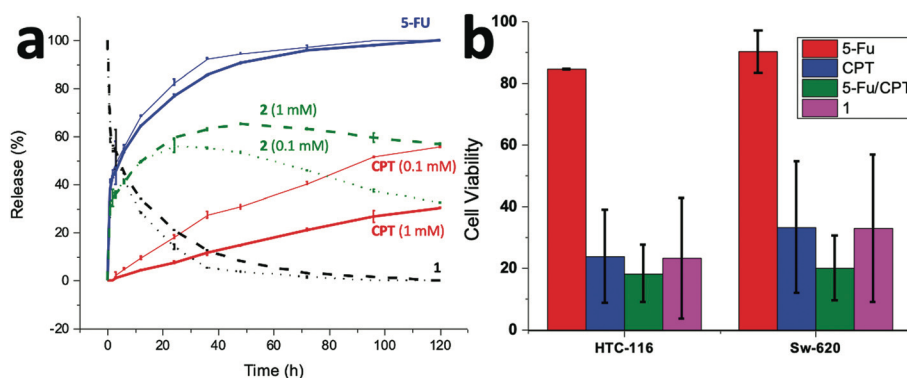


Fig. 4 (a) Release of free CPT (red) and 5-FU (blue), and breakdown/formation of **1** (black) and **2** (green), as monitored by HPLC, from nanotubes of **1** in PBS at 37.5 at 0.1 (thin lines) and 1 mM (thick lines) over 120 h. (b) MTT cytotoxicity assay comparing 5-FU, CPT, 5-FU/CPT and **1** activities against human non-small cell lung cancer cell lines H116 and SW620.

2 to remain assembled into nanotubes following 5-FU release, with similar dimensions to those of **1**. Imaging the nanotubes as the drugs were released by TEM over time in PBS at 37 °C showed regions with abrupt decreases in diameters from ~90 to 77 nm, consistent with the dimensions measured for nanotubes formed by **1** and **2**, respectively (Fig. 3b, S20†). Similar changes in cross-sectional heights could be observed by AFM after 24 h at 37 °C (Fig. 3c, S21†). These presence of these steps in diameter suggested that hydrolytic erosion of the nanotube surface produced another slightly smaller nanotube, derived from **2**, that persisted after initial release of 5-FU.

The dual drug nanotube (**1**) was assessed for efficacy against human non-small cell lung cancer (NSCLC) cell lines H116 and SW620 and was compared to CPT, 5-FU and the combined solution of 5-FU and CPT. The cytotoxic activity was assayed using an MTT-assay over the course of a 96 h incubation period to determine cell viability. Peptide **1** exhibited significantly higher cytotoxicity than 5-FU alone, due to the presence of CPT in the conjugate, and similar efficacy as CPT alone or as a combination with 5-FU, against both cell lines. Further studies will be required to evaluate the ability of this dual-drug construct to reduce systemic toxicity and drug resistance *in vivo*.

Conclusions

We have described a dual-drug, peptide nanotube that sequentially released free 5-FU and CPT in PBS and showed efficacy against two human lung cancer cell lines. The nanotube vehicle was created by the self-assembly of **1** in aqueous media, which positioned the hydrophilic 5-FU molecule at the surface of the nanotube and sequestered CPT within the hydrophobic nanotube walls. This structural feature caused the release profiles of the two drugs to be distinct. Accordingly, a rapid release of 5-FU was followed by the slower, sustained production of CPT. The slower, sustained release profile of CPT was maintained by the persistence of nanotubes of peptide **2**, which were produced from **1** upon hydrolytic release of 5-FU. The ability to design self-assembled drug carriers that remain assembled after initial drug releases should facilitate the development of new strategies for delivering combination therapy.

Conflicts of interest

There are no conflicts to declare.

Notes and references

- J. Xiang, X. Liu, G. Yuan, R. Zhang, Q. Zhou, T. Xie and Y. Shen, Nanomedicine from amphiphilized prodrugs: Concept and clinical translation, *Adv. Drug Delivery Rev.*, 2021, **179**, 114027.

- M. S. Yoon, Y. J. Lee, H. J. Shin, C. W. Park, S. B. Han, J. K. Jung, J. S. Kim and D. H. Shin, Recent Advances and Challenges in Controlling the Spatiotemporal Release of Combinatorial, Anticancer Drugs from Nanoparticles, *Pharmaceutics*, 2020, **12**, 12121156.
- H. Maeda, J. Wu, T. Sawa, Y. Matsumura and K. Hori, Tumor vascular permeability and the EPR effect in macromolecular therapeutics: a review, *J. Controlled Release*, 2000, **65**, 271–284.
- W. T. Huang, M. Larsson, Y. C. Lee, D. M. Liu and G. Y. Chiou, Dual drug-loaded biofunctionalized amphiphilic chitosan nanoparticles: Enhanced synergy between cisplatin and demethoxycurcumin against multidrug-resistant stem-like lung cancer cells, *Eur. J. Pharm. Biopharm.*, 2016, **109**, 165–173.
- W. Ni, Z. Li, Z. Liu, Y. Ji, L. Wu, S. Sun, X. Jian and X. Gao, Dual-Targeting Nanoparticles: Codelivery of Curcumin and 5-Fluorouracil for Synergistic Treatment of Hepatocarcinoma, *J. Pharm. Sci.*, 2019, **108**, 1284–1295.
- Z. Gao, Z. Li, J. Yan and P. Wang, Irinotecan and 5-fluorouracil-co-loaded, hyaluronic acid-modified layer-by-layer nanoparticles for targeted gastric carcinoma therapy, *Drug Des., Dev. Ther.*, 2017, **11**, 2595–2604.
- J. E. Cortes, S. L. Goldberg, E. J. Feldman, D. A. Rizzi, D. E. Hogge, M. Larson, A. Pigneux, C. Recher, G. Schiller, K. Warzocha, H. Kantarjian, A. C. Louie and J. E. Kolitz, Phase II, multicenter, randomized trial of CPX-351 (cytarabine:daunorubicin) liposome injection versus intensive salvage therapy in adults with first relapse AML, *Cancer*, 2015, **121**, 234–242.
- X. Zhang, W. Zong, J. Wang, M. Dong, W. Cheng, T. Sun and X. Han, Multicompartmentalized vesosomes containing DOX loaded liposomes and 5FU loaded liposomes for synergistic tumor treatment, *New J. Chem.*, 2019, **43**, 4895–4899.
- L. Zhang, A. F. Radovic-Moreno, F. Alexis, F. X. Gu, P. A. Basto, V. Bagalkot, S. Jon, R. S. Langer and O. C. Farokhzad, Co-delivery of hydrophobic and hydrophilic drugs from nanoparticle-aptamer bioconjugates, *ChemMedChem*, 2007, **2**, 1268–1271.
- S. Gadde, Multi-drug delivery nanocarriers for combination therapy, *MedChemComm*, 2015, **6**, 1916–1929.
- P. Kesharwani, K. Jain and N. K. Jain, Dendrimer as nanocarrier for drug delivery, *Prog. Polym. Sci.*, 2014, **39**, 268–307.
- S. Aryal, C. M. Hu and L. Zhang, Combinatorial drug conjugation enables nanoparticle dual-drug delivery, *Small*, 2010, **6**, 1442–1448.
- D. Wu, Y. Chen, S. Wen, Y. Wen, R. Wang, Q. Zhang, G. Qin, H. Yi, M. Wu, L. Lu, X. Tao and X. Deng, Synergistically Enhanced Inhibitory Effects of Pullulan Nanoparticle-Mediated Co-Delivery of Lovastatin and Doxorubicin to Triple-Negative Breast Cancer Cells, *Nanoscale Res. Lett.*, 2019, **14**, 314.
- C. Gao, P. Bhattacharai, M. Chen, N. Zhang, S. Hameed, X. Yue and Z. Dai, Amphiphilic Drug Conjugates as

Nanomedicines for Combined Cancer Therapy, *Bioconjugate Chem.*, 2018, **29**, 3967–3981.

15 I. W. Hamley, Small Bioactive Peptides for Biomaterials Design and Therapeutics, *Chem. Rev.*, 2017, **117**, 14015–14041.

16 J. Wu, W. Ding, G. Han, W. You, W. Gao, H. Shen, J. Tang, Q. Tang and X. Wang, Nuclear delivery of dual anti-cancer drugs by molecular self-assembly, *Biomater. Sci.*, 2021, **9**, 116–123.

17 T. Xu, C. Liang, D. Zheng, X. Yan, Y. Chen, Y. Chen, X. Li, Y. Shi, L. Wang and Z. Yang, Nuclear delivery of dual anti-cancer drug-based nanomedicine constructed by cisplatin-induced peptide self-assembly, *Nanoscale*, 2020, **12**, 15275–15282.

18 X. Wang, X. Cheng, L. He, X. Zeng, Y. Zheng and R. Tang, Self-Assembled Indomethacin Dimer Nanoparticles Loaded with Doxorubicin for Combination Therapy in Resistant Breast Cancer, *ACS Appl. Mater. Interfaces*, 2019, **11**, 28597–28609.

19 K. Cheng, Y. Ding, Y. Zhao, S. Ye, X. Zhao, Y. Zhang, T. Ji, H. Wu, B. Wang, G. J. Anderson, L. Ren and G. Nie, Sequentially Responsive Therapeutic Peptide Assembling Nanoparticles for Dual-Targeted Cancer Immunotherapy, *Nano Lett.*, 2018, **18**, 3250–3258.

20 R. Zhang, R. Xing, T. Jiao, K. Ma, C. Chen, G. Ma and X. Yan, Carrier-Free, Chemophotodynamic Dual Nanodrugs via Self-Assembly for Synergistic Antitumor Therapy, *ACS Appl. Mater. Interfaces*, 2016, **8**, 13262–13269.

21 H. Cao, Y. Yang, X. Chen and Z. Shao, Intelligent Janus nanoparticles for intracellular real-time monitoring of dual drug release, *Nanoscale*, 2016, **8**, 6754–6760.

22 M. Hu, P. Huang, Y. Wang, Y. Su, L. Zhou, X. Zhu and D. Yan, Synergistic Combination Chemotherapy of Camptothecin and Floxuridine through Self-Assembly of Amphiphilic Drug-Drug Conjugate, *Bioconjugate Chem.*, 2015, **26**, 2497–2506.

23 P. Huang, D. Wang, Y. Su, W. Huang, Y. Zhou, D. Cui, X. Zhu and D. Yan, Combination of small molecule prodrug and nanodrug delivery: amphiphilic drug-drug conjugate for cancer therapy, *J. Am. Chem. Soc.*, 2014, **136**, 11748–11756.

24 A. Gitsas, G. Floudas, M. Mondeshki, I. Lieberwirth, H. W. Spiess, H. Iatrou, N. Hadjichristidis and A. Hirao, Hierarchical Self-Assembly and Dynamics of a Miktoarm StarchimeraComposed of Poly(γ -benzyl-L-glutamate), Polystyrene, and Polyisoprene, *Macromolecules*, 2010, **43**, 1874–1881.

25 R. A. Ribeiro, C. W. Wanderley, D. V. Wong, J. M. Mota, C. A. Leite, M. H. Souza, F. Q. Cunha and R. C. Lima-Junior, Irinotecan- and 5-fluorouracil-induced intestinal mucositis: insights into pathogenesis and therapeutic perspectives, *Cancer Chemother. Pharmacol.*, 2016, **78**, 881–893.

26 L. B. Saltz, J.-Y. Douillard, N. Pirotta, M. Alakl, G. Gruia, L. Awad, G. L. Elfring, P. K. Locker and L. L. Miller, Irinotecan Plus Fluorouracil/Leucovorin for Metastatic Colorectal Cancer: A New Survival Standard, *Oncologist*, 2001, **6**, 81–91.

27 E. Samalin, P. Afchain, S. Thézenas, F. Abbas, O. Romano, R. Guimbaud, Y. Bécouarn, F. Desseigne, J. Edeline, E. Mitry, O. Bouché, A. Adenis, T. Aparicio, E. Dorval, A. Kramar and M. Ychou, Efficacy of irinotecan in combination with 5-fluorouracil (FOLFIRI) for metastatic gastric or gastroesophageal junction adenocarcinomas (MGA) treatment, *Clin. Res. Hepatol. Gastroenterol.*, 2011, **35**, 48–54.

28 Y. Sun, A. Shieh, S. H. Kim, S. King, A. Kim, H.-L. Sun, C. M. Croce and J. R. Parquette, The self-assembly of a camptothecin-lysine nanotube, *Bioorg. Med. Chem. Lett.*, 2016, **26**, 2834–2838.

29 Y. Sun, J. A. Kaplan, A. Shieh, H.-L. Sun, C. M. Croce, M. W. Grinstaff and J. R. Parquette, Self-assembly of a 5-fluorouracil-dipeptide hydrogel, *Chem. Commun.*, 2016, **52**, 5254–5257.

30 S. H. Kim, J. A. Kaplan, Y. Sun, A. Shieh, H. L. Sun, C. M. Croce, M. W. Grinstaff and J. R. Parquette, The Self-Assembly of Anticancer Camptothecin-Dipeptide Nanotubes: A Minimalistic and High Drug Loading Approach to Increased Efficacy, *Chem. – Eur. J.*, 2015, **21**, 101–105.

31 F. Wurthner, T. E. Kaiser and C. R. Saha-Moller, J-aggregates: from serendipitous discovery to supramolecular engineering of functional dye materials, *Angew. Chem., Int. Ed.*, 2011, **50**, 3376–3410.

32 T. Miyazawa and E. R. Blout, Infrared Spectra of Polypeptides in Various Conformations - Amide I and II Bands, *J. Am. Chem. Soc.*, 1961, **83**, 712–719.

33 R. Lin, A. G. Cheetham, P. Zhang, Y. A. Lin and H. Cui, Supramolecular filaments containing a fixed 41% paclitaxel loading, *Chem. Commun.*, 2013, **49**, 4968–4970.

34 G. Chirico, M. Collini, F. Olivini, M. Zamai, E. Frigerio and V. R. Caiolfa, Aggregation properties of a HPMA-camptothecin copolymer in isotonic solutions, *Biophys. Chem.*, 2004, **110**, 281–295.

35 T. W. B. Cai, X. P. Tang, J. Nagorski, P. G. Brauschweiger and P. G. Wang, Synthesis and cytotoxicity of 5-fluorouracil/diazeniumdiolate conjugates, *Bioorg. Med. Chem.*, 2003, **11**, 4971–4975.

36 L. Ouyang, D. S. He, J. Zhang, G. He, B. Jiang, Q. Wang, Z. J. Chen, J. Z. Pan, Y. H. Li and L. Guo, Selective bone targeting 5-fluorouracil prodrugs: Synthesis and preliminary biological evaluation, *Bioorg. Med. Chem.*, 2011, **19**, 3750–3756.